





16 **Abstract:** The soil organic carbon pool is a crucial component of carbon storage in terrestrial ecosystems, playing a key role  
17 in regulating the carbon cycle and mitigating atmospheric CO<sub>2</sub> concentration increases. To combat soil degradation and  
18 enhance soil organic carbon sequestration on the Loess Plateau, the Grain-for-Green Program (GFGP) has been implemented.  
19 Accurately quantifying carbon capture and storage (CCS) resulting from farmland retirement is essential for informing land  
20 use management. In this study, the spatial and temporal distribution of retired farmlands on the Loess Plateau was analyzed  
21 using Landsat imagery from 1999 to 2021. To assess the effects of the length of farmland retirement, climate, soil properties,  
22 elevation, and other factors on CCS, climate-zone-specific linear regression models were developed based on field-sampled  
23 soil data. These models were then used to map the dataset of CCS across the retired farmlands. Results indicate that a total of  
24 39,065 km<sup>2</sup> of farmland was retired over the past two decades, with 45.61% converted to grasslands, 29.75% to shrublands,  
25 and 24.64% to forestlands. The length of farmland retirement showed a significant positive correlation with CCS, and  
26 distinct models were developed for different climatic zones to achieve high-resolution (30 m) CCS mapping. The total CCS  
27 from retired farmland on the Loess Plateau was estimated at 21.77 Tg in carbon equivalent according to the dataset, with  
28 grasslands contributing 81.10%, followed by forestlands (11.16%) and shrublands (7.74%).

29 **Keywords:** Length of farmland retirement; carbon capture and storage; ecological restoration; land use change;  
30 grain-for-green

31  
32



### 33 1. Introduction

34 Soil organic carbon (SOC), as the largest terrestrial ecosystem carbon pool, plays a crucial role in regulating climate  
35 change (Mir et al., 2023). Global SOC was estimated at approximately 1,400-1,500 Pg C, about four times the organic  
36 carbon pool of terrestrial plants (Scharlemann et al., 2014). The high SOC is essential to support multiple ecological benefits,  
37 such as purifying water, increasing crop yields and maintaining primary productivity (Paustian et al., 2019). Currently, 1/3  
38 soil in the world is degraded, causing many socioeconomic (e.g., unemployment, poverty, immigration) and environmental  
39 (e.g., desertification, ecosystem degradation, biodiversity loss) issues (Ferreira et al., 2022; Ouyang et al., 2016). The large  
40 area of degraded soil also released more than 50 Pg carbon per year into the atmosphere which is conflict to the  
41 decarbonization target for mitigating global warming (Právělie et al., 2021). Therefore, the restoration of degraded soil is  
42 urgently needed for sustainable development and environment safety.

43 Ecological restoration by nature alone is a lengthy process. Under the urgent need for restoring degraded soils and  
44 mitigating climate change, scientific management measures are necessary to accelerate the ecosystem restoration (Lengefeld  
45 et al., 2020; Pape, 2022; Wang et al., 2021a). Many large-scale ecological restoration strategies around the world have  
46 showed encouraging ecological benefits. Brazil's Atlantic Forest Restoration Pact (AFRP) was established in 2009, and  
47 Argentina and Paraguay joined the impressive project in 2018, forming the Atlantic Forest Restoration Tri-national Network  
48 (Calmon et al., 2011). Hundreds of organizations have been actively involved in this decade-long efforts to protect and  
49 restore the forest, which recovered about 7,000 km<sup>2</sup> forest and enhanced regional biodiversity (De Oliveira Faria and  
50 Magrini, 2016). Forests established by restoration of the Brazilian Atlantic Forest between 2010 and 2015 would have  
51 sequestered 1.75 Pg carbon if they were not re-cut (Piffer et al., 2022). The Development Project "Green Great Wall" in  
52 Africa was launched by the African Union in 2007, aiming at restoring savannahs, grasslands and farmlands across Africa to  
53 help biodiversity cope with climate change and desertification. The goals of the project are to restore 1,000,000 km<sup>2</sup> in 2030  
54 and sequester 250 Tg C (Graham, 2022; Macia et al., 2023). China has started ecological restoration practices and researches  
55 since the 1970s, and has implemented six national key ecological restoration projects (Cui et al., 2021). Among the projects,  
56 the GFGP is one of the most ambitious projects in the world with the highest investment and the largest implemented area  
57 (Xu et al., 2022). From 1999 to 2019, the GFGP implemented in 25 provinces and exceeded 0.343 million km<sup>2</sup> land area  
58 with 49 Tg sequestered carbon, indicating a significant potential of carbon capture and storage (CCS) by ecological  
59 restoration (Lu et al., 2018). Based on Deng et al.'s (2017)(Deng et al., 2017) study, the total carbon stock in the GFGP  
60 affected area was 682 Tg C in 2010, and projected to 1,697 Tg C in 2020.

61 One of the primary area of the GFGP is the Loess Plateau, because the long-term indiscriminate cultivation and logging  
62 on the Loess Plateau has caused over 40% of the total area (about 270,000 km<sup>2</sup>) in severe soil erosion and a significant loss  
63 of organic carbon (Shao et al., 2022). As the implementation of the GFGP, 96.1 Tg C was sequestered from 2000 to 2008 on  
64 the Loess Plateau (Feng et al., 2013; Xiao, 2014). Nonetheless, current estimations of CCS still have large uncertainties due  
65 to the technology and data limits (Zhang et al., 2022). On the Loess Plateau, the accumulation of SOC can be affected by  
66 many untested factors, such as ecosystem types and length of farmland retirement. Moreover, most of the studies fail to  
67 differentiate the carbon sequestration between retired and in use farmlands, and caused an overestimate of CCS. Therefore, a  
68 more reliable estimation should be reached to quantify the CCS of the retired farmlands with the consideration of those  
69 issues (Deng et al., 2017; Sun et al., 2016).

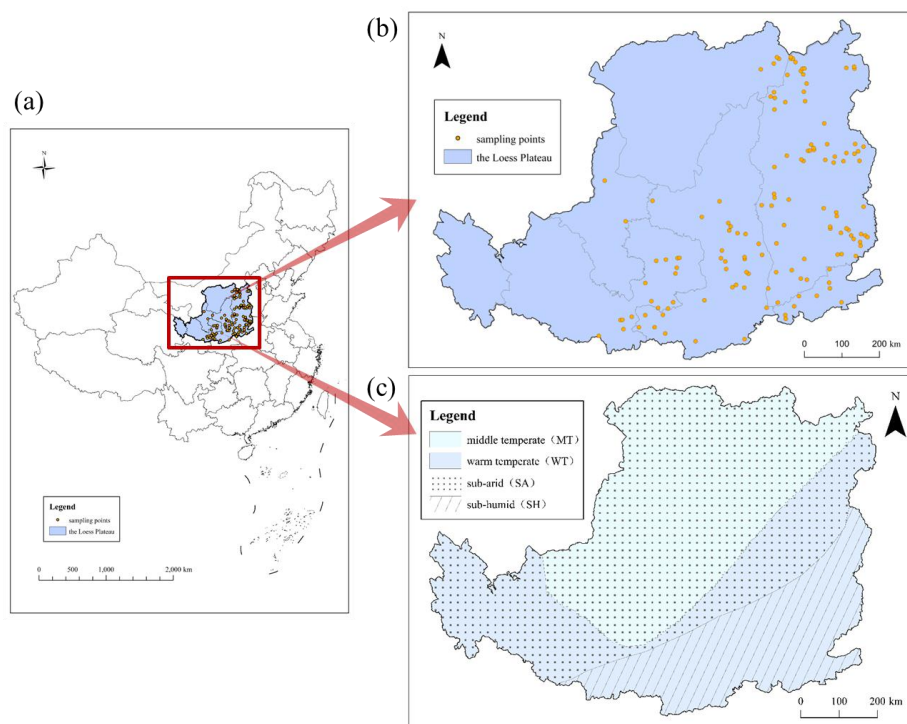


70 Regarding to the complex spatial heterogeneity on the Loess Plateau and long-time implementation of the GFGP (Ma et  
71 al., 2022), the change of SOC in high resolution since the implementation of the GFGP is essential to clarify the CCS from  
72 large-scale ecological restoration, and can provide scientific guidance for ecological restoration policy and land use  
73 management on the Loess Plateau and sustainable utilization of vegetation resources. With the advancing of remote sensing  
74 technology and well-designed sample scheme, the objectives of this study are: 1) to identify the year-by-year retirement of  
75 farmlands on the Loess Plateau from 2000 to 2021; 2) to develop models of CCS for the retired farmlands contributed by the  
76 GFGP; 3) to map the CCS in 30 m resolution and estimate the total CCS from the retired farmlands on the Loess Plateau  
77 after the implementation of the GFGP.

## 78 2. Materials and Methods

### 79 2.1 Study Area

80 The Loess Plateau (100° 52'–114° 33' E, 33° 41'–41° 16' N) is located in the north central part of China (Fig. 1-a), in  
81 the middle reaches of the Yellow River, with a sensitive and fragile ecological environment, belonging to the warm  
82 temperate continental monsoon climate, characterized by dry and cold in spring and winter, warm and hot in summer and  
83 autumn (Ma et al., 2022). The average annual temperature is 3.6–14.3°C. The average annual precipitation is 400–600 mm,  
84 of which is concentrated between July and September, and decreases from east to west and south to north (Zhou et al., 2016).  
85 The annual evaporation is 1,400–2,100 mm, with a trend of low in the south and east, high in the north and west. The  
86 elevation is 800–3,000 m, and the original surface vegetation mostly is grassland, shrubland, deciduous broadleaf forest, and  
87 mixed broadleaf-conifer forest (Zhou et al., 2016). The total area of the Loess Plateau is 635,000 km<sup>2</sup>, including Shanxi,  
88 Ningxia, Shaanxi, Gansu, Qinghai, Inner Mongolia, Henan provinces. The main terrain is hilly and gully, with soft loessial  
89 soil texture.





91 **Figure 1. The map of the study area, (a) location, (b) soil sampling sites and (c) climate zones.**

92 2.2 Identifying Retired Farmlands

93 To identify and confirm the spatial range of the annual retired farmlands on the Loess Plateau, Landsat remote sensing  
94 images (30 m resolution) from 1999 to 2021 were downloaded from the United States Geological Survey (USGS,  
95 <https://EarthExplorer.usgs.gov>). The images with less cloud (lower than 10%) in growing season (from May to September)  
96 were selected for further analysis. Those images were processed by the standard steps recommended by ArcGIS Pro 2.8  
97 (Environmental Systems Research Institute, Inc., ESRI), including preprocessing, image classification and validation. To  
98 improve image readability, remote sensing images were first preprocessed in ENVI 5.3, including radiometric calibration,  
99 FLAASH (Fast Line-of-sight Atmospheric Analysis of Spectral Hypercubes) atmospheric correction, gram-schmidt pan  
100 sharpening, seamless mosaic and subset data from ROIs (regions of interest). The image classification was then performed in  
101 ArcGIS Pro 2.8. In this study, we used the support vector machine (SVM) supervised classification method to classify the  
102 land cover types into the following seven categories: farmland, forestland, grassland, shrubland, water body, building land,  
103 and bare land. The training samples were selected by visual interpretation and managed by training sample manager. In the  
104 accuracy validation stage, the kappa coefficients for the studied period were in a range of 0.76–0.90 and the overall  
105 accuracy were 0.80–0.91 for different land cover types.

106 2.3 Field Sampling and SOC Measurements

107 To determine the CCS of different ecosystems that established on retired farmlands, an initial set of sample sites were  
108 created evenly with 5 km gaps based on the spatial distribution maps of retired farmlands (Fig. 1-b), and the final sample  
109 sites were determined by removing unqualified sites with ultra-high spatial resolution images (0.5 m resolution). Finally,  
110 2,430 soil samples from 135 sample sites were collected from fields. Nine soil samples (three 10-cm layers from top 30 cm  
111 soil in 3 sample points) were collected for every sample site, and nine soil samples from the nearest farmlands were also  
112 collected similarly. Each soil sample was individually bagged, labeled, and stored in cold storage for lab measurement. After  
113 drying and grinding through a sieve at 0.25 mm, SOC of each soil sample was measured by potassium dichromate external  
114 heating method. The difference in total SOC of the top 30 cm soil layer between retired farmlands and the nearest farmlands  
115 was defined as CCS that contributed by the GFGP.

116 2.4 Model Development and CCS Mapping on the Loess Plateau

117 CCS is influenced by both natural environmental conditions and human activities, leading to variations across different  
118 zones of the Loess Plateau. Therefore, we developed different models based on the relationships between CCS and variables  
119 such as length of farmland retirement, geographic location, elevation, soil bulk density (BD), temperature, precipitation, and  
120 19 bioclimatic factors. Length of farmland retirement were obtained from the annual spatial distribution data in retired  
121 farmlands on the Loess Plateau (subsection 2.2). The data sources for climate information can be found in subsection 2.5.  
122 The 19 bioclimatic factors were derived by following the formula in WorldClim (<https://worldclim.org/data/index.html>). All  
123 the variables were extracted to the sample sites by the Kriging interpolation and prepared for model development.

124 Based on the factors introduced above, we combined correlation analysis, random forest and single-factor regression to  
125 select variables for multivariate linear models of CCS. In consideration of wide climatic range on the Loess Plateau and  
126 different possible response of CCS to the retirement factors among climatic conditions (Zhang et al., 2018), we divided the  
127 Loess Plateau into different climatic zones for different ecosystem types (e.g., forestland, shrubland, grassland) based on



128 climate regionalization in China—Climatic zones and climatic regions (GB/T 17297-1998) and climate data (subsection 2.5).  
129 As Fig. 1-c shows, we obtained middle temperature zone (MT,  $< 8^{\circ}\text{C}$ ) and warm temperate zone (WT,  $> 8^{\circ}\text{C}$ ) by the annual  
130 average temperature, and semi-arid zone (SA,  $< 400\text{ mm}$ ) and sub-humid zone (SH,  $> 400\text{ mm}$ ) by annual precipitation. In  
131 addition, three combined climatic zones were obtained: MT-SA, WT-SA and WT-SH. A multivariate linear regression model  
132 was developed specifically for each ecosystem types in each climatic zone. Before regression analysis, diagnosis of  
133 multicollinearity is conducted, and the threshold is generally set at 10 to detecting correlations between the independent  
134 variables and identify those independent variables that were incorrectly included in the same regression model. The  
135 regression models were evaluated and validated by residual analysis, cross-validation, significance level ( $p$ -value),  
136 coefficient of determination ( $R^2$ ), root mean square error (RMSE) and mean absolute error (MAE).

137 Based on the results of model evaluation, the best fitted models were selected to estimate the overall CCS of retired  
138 farmlands on the Loess Plateau. With the final selected multivariate linear regression models, the CCS in the top 30 cm soil  
139 layer were mapped by raster calculation in different climatic zones and ecosystem types at 30 m resolution. And the total  
140 CCS on the Loess Plateau contributed by the GFGP was obtained by summing up the CCS in all the retired farmlands  
141 without reclamation within the study period.

#### 142 2.5 Data Sources

143 The temperature and precipitation data to calculate the 19 bioclimatic factors were from the China Meteorological Data  
144 Service Center (CMDC, <http://www.geodata.cn>). Elevation data of every grid cell were from the Digital Elevation Model  
145 database (<https://e4ftl01.cr.usgs.gov/MEASURES/>). Soil properties were retrieved from Harmonized World Soil Database  
146 (HWSD, <https://www.fao.org/soils-portal/soil-survey/soil-maps-and-databases/harmonized-world-soil-database-v12/en/>),  
147 and the boundary of the Loess Plateau was downloaded from the Resource and Environment Science and Data Center  
148 (<https://www.resdc.cn/>). All the raster data were resampled to 30 m resolution.

### 149 3. Results

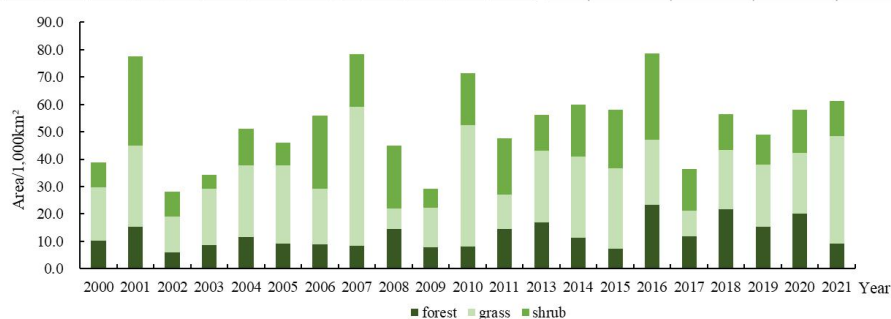
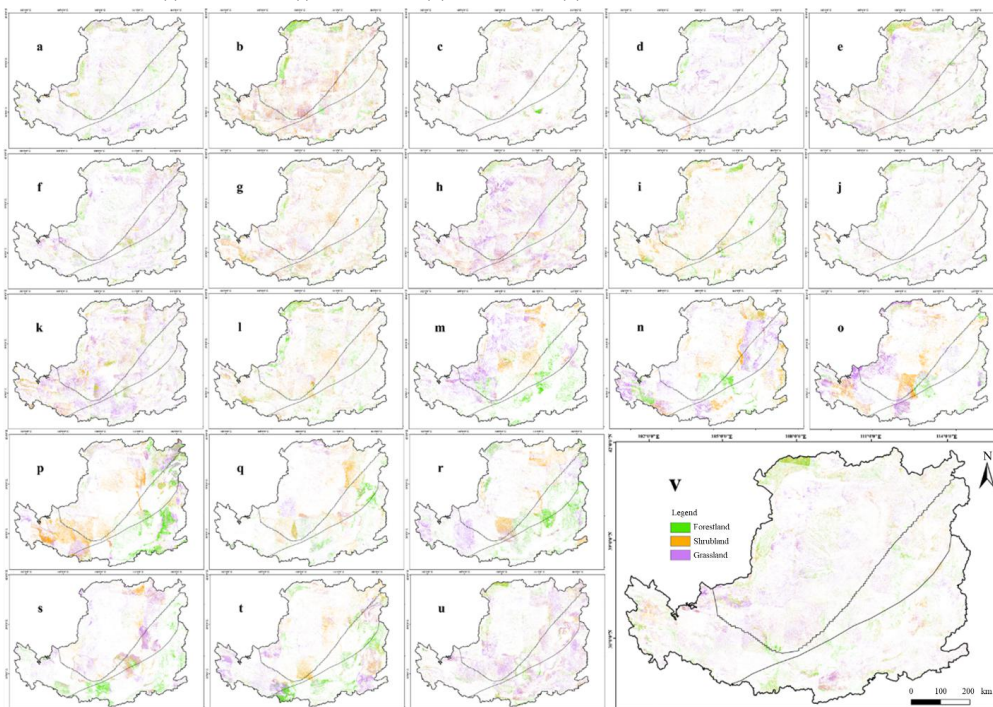
#### 150 3.1 Distribution of Retired Farmlands

151 From 1999 to 2021, the final retired farmlands without reclamation on the Loess Plateau was  $39,065\text{ km}^2$  (Fig. 2 v). The  
152 final retired farmlands were less than the area by summing up yearly retired farmlands because of frequent reclamation. The  
153 area of retired farmlands in every year has been fluctuating throughout the study period with no significant trend (Fig 2 a-u,  
154 Fig. 3). The least amount of retired farmlands occurred in 2002 ( $28,003\text{ km}^2$ ; 4.41% of the whole studied area), and the most  
155 was  $78,653\text{ km}^2$  in 2016 (12.39% of the whole studied area). The retired farmlands were converted to different ecosystem  
156 types, including forestlands, shrublands and grasslands. The ratios of different ecosystem types in every year were in the  
157 ranges of 10.65%–38.60%, 14.63%–47.70% and 17.02%–64.98% for forestlands, shrublands and grasslands, respectively



158 (Fig. 3). Within the studied period in average, most of the retired farmlands were converted to grasslands (45.61 %) and  
 159 shrublands (29.75 %).

160 **Figure 2. Spatial distribution of retired farmlands on the Loess Plateau from 1999 to 2021, (a) 1999-2000, (b)**  
 161 **2000-2001, (c) 2001-2002, (d) 2002-2003, (e) 2003-2004, (f) 2004-2005, (g) 2005-2006, (h) 2006-2007, (i) 2007-2008, (j)**  
 162 **2008-2009, (k) 2009-2010, (l) 2010-2011, (m) 2011-2013, (n) 2013-2014, (o) 2014-2015, (p) 2015-2016, (q) 2016-2017, (r)**  
 163 **2017-2018, (s) 2018-2019, (t) 2019-2020, (u) 2020-2021, (v) 1999-2021.**



164 **Figure 3. Area of**  
 165 **different ecosystem types from retired farmlands from 2000 to 2021.**

166 The retired farmlands were unevenly distributed among different climate zones (Fig. 2 a-v). For the final retired  
 167 farmlands, the area in the middle temperate and semi-arid zone (MT-SA), warm temperature and semi-arid zone (WT-SA)  
 168 and warm-temperature and semi-humid zone (WT-SH) were 20,299 km<sup>2</sup>, 10,572 km<sup>2</sup> and 8,194 km<sup>2</sup>, respectively. In the  
 169 MT-SA zone, the dominant ecosystem type from retired farmlands was grasslands which had 9,705 km<sup>2</sup> (47.81%), and  
 170 followed by shrublands (5,887 km<sup>2</sup>, 29.00%) and forestlands (4,707 km<sup>2</sup>, 23.19%). In the WT-SA zone, grasslands were also  
 171 the dominant ecosystem type which accounted for 4,925 km<sup>2</sup> (46.59%), and forestlands accounted the least (2,384 km<sup>2</sup>,  
 172 22.55%). In the WT-SH zone, the percentages of different ecosystem types were 30.96 %, 30.16 % and 38.88 % for



173 forestlands, shrublands and grasslands, respectively.

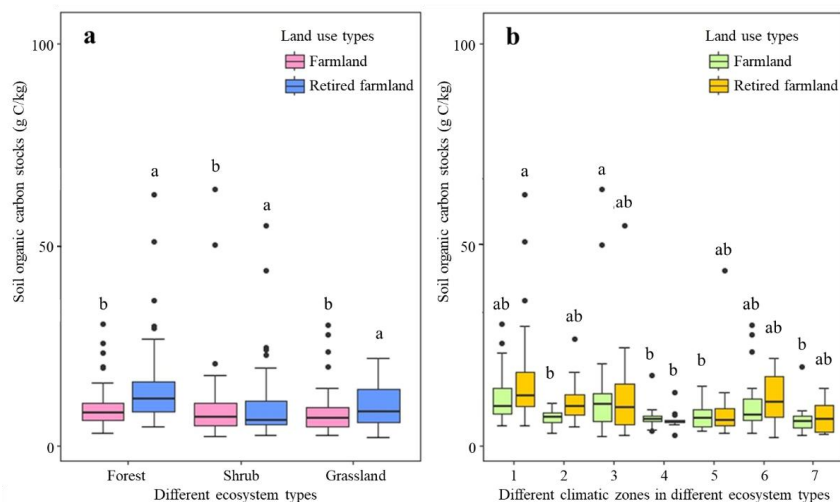
174 Among different years (Fig. 2 a-u), the highest areas for each ecosystem type were forestlands in the WT-SH zone in  
175 2016 (12,846 km<sup>2</sup>), shrublands in the MT-SA zone in 2001 (15,441 km<sup>2</sup>), and grasslands in the MT-SA zone in 2007 (26,171  
176 km<sup>2</sup>). The lowest areas were found in 2019 for forestlands in the WT-SA zone (813 km<sup>2</sup>), in 2013 for shrublands in the  
177 WT-SH zone (271 km<sup>2</sup>), and in 2013 for grasslands in the WT-SH zone (806 km<sup>2</sup>).

178 Among provinces, the retired farmlands in different years had significant differences (Table S1), where Shanxi Province  
179 had the most in 2016 (30,912 km<sup>2</sup>) and Qinghai Province had the least in 2017 (438 km<sup>2</sup>). The final retired farmlands from  
180 1999-2021 was the most in Inner Mongolia Province (8,626 km<sup>2</sup>) and the least in Henan Province (739 km<sup>2</sup>). More  
181 forestlands could be found in warmer and wetter regions. The largest forestlands (15,073 km<sup>2</sup>) were found in Shanxi  
182 Province in 2016, while the least were found in Qinghai Province in 2016 (34 km<sup>2</sup>).

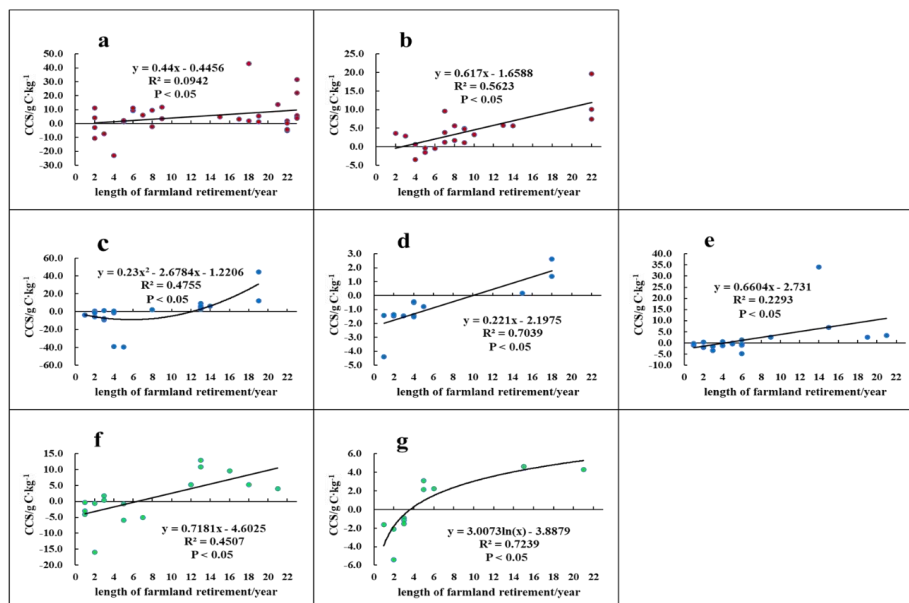
### 183 3.2 Analysis of Soil Samples

184 The results of soil samples showed that the SOC were 2.19–62.70 g C/kg in retired farmlands, and 2.25–63.83 g C/kg in  
185 adjacent farmlands. The average SOC were the highest in forestlands (4.84–62.70 g C/kg), followed by shrublands  
186 (2.62–54.72 g C/kg) and grasslands (2.19–21.83 g C/kg). To facilitate the CCS estimation by area, we converted the SOC to  
187 area based content by soil bulk density. The highest value of CCS after retirement was from forestlands in the SH zone  
188 (26.52 kg C/m<sup>2</sup>) and the lowest value was from sample in grasslands in the WT zone (0.91 kg C/m<sup>2</sup>). Forestlands and  
189 shrublands had significantly increased the SOC by 48.53% and 20.34%, respectively ( $p < 0.05$ , Fig. 4 a). Among different  
190 climatic zones (Fig. 4 b), forestlands in the SA zone had the biggest increase (58.80%), and followed by forestlands in the  
191 SH zone (44.53%) and shrublands in the MT-SA zone (26.74%). The findings indicated that the farmland retirement had  
192 significantly increased the SOC storage.

193 The CCS of different ecosystem types in different climatic zones had significant relationship to the length of farmland  
194 retirement (Fig. 5). The CCS was negative in the first few years and significantly increased as the length of farmland  
195 retirement increases, except forestlands in the SA zone and shrublands in the MT-SA zone. Most of the relationships  
196 indicated constant increase in CCS except CCS in grasslands in the MT zone which had a saturation point after 15 years of  
197 retirement.





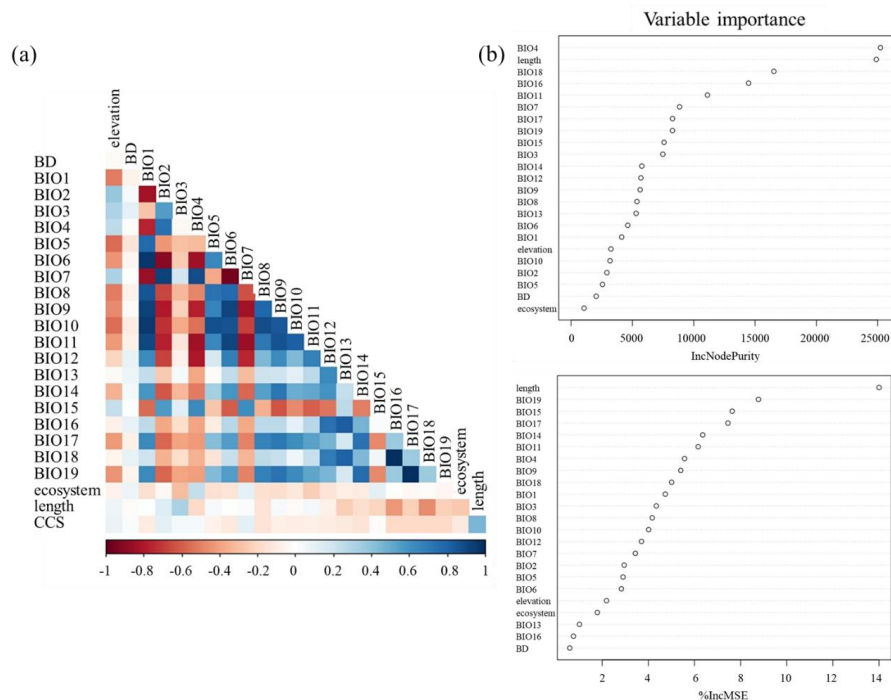


206 **Figure 5. Relationship between length of farmland retirement and CCS, (a) forestlands in the SH zone, (b)**  
 207 **forestlands in the SA zone, (c) shrublands in the WT-SH zone, (d) shrublands in the WT-SA zone, (e) shrublands**  
 208 **in the MT-SA zone, (f) grasslands in the WT zone, (g) grasslands in the MT zone.**

209 3.3 Models of CCS

210 3.3.1 Correlation analysis and variable importance

211 The critical variables for model development were selected by the Pearson correlation analysis and variable importance  
 212 through package *randomForest* in R. The length of farmland retirement and CCS (Fig. 6 a) showed a significant positive  
 213 correlation. Most of the environmental factors such as soil bulk density and bioclimatic factors had a weak negative  
 214 correlation with CCS. Variable importance (Fig. 6 b) was measured in %IncMSE (percent increase in mean squared error)  
 215 and IncNodePurity (increase in node purity). The combination of the two metrics illustrated that the length of farmland  
 216 retirement on the Loess Plateau is the most important variable for CCS.  
 217



218  
 219 **Figure 6. Correlation matrix (a) and variable importance (b) of CCS and environmental factor parameters.**

220 3.3.2 Model development

221 Based on the results from correlation analysis and variable importance, all the factors significant contributing to the  
 222 variance of CCS were introduced into the regression model. Samples for different ecosystem types were divided by different  
 223 combinations of climatic zones to find the optimal model by Backward Stepwise Regression. The final models of CCS in  
 224 different ecosystem types were shown in Table 1. In this table, *t* is the length of farmland retirement, *lat* is latitude, *ele* is  
 225 elevation, *BD* is soil bulk density, and *BIO1*-*BIO19* are 19 bioclimatic factors.

226 The analysis showed that seven regression equations were the best representative for the CCS on the Loess Plateau  
 227 when the study area was divided into SH and SA zones for forestlands, WT-SH, WT-SA and MT-SA zones for shrublands,  
 228 and WT and MT zones for grasslands. The coefficients of determination ( $R^2$ ) ranged from 0.476 to 0.830 with  $p < 0.05$ . The  
 229 models with the highest  $R^2$  were obtained for grasslands (0.830 in the WT zone and 0.790 in the MT zone), and the model  
 230 with the lowest  $R^2$  was for shrublands in the MT zone (0.476).

231  
 232  
 233

**Table 1 Models of the CCS in retired farmlands on the Loess Plateau.**

Ecosystem	Zone	Model	$R^2$	<i>p</i> -value	RMSE	MAE
-----------	------	-------	-------	-----------------	------	-----

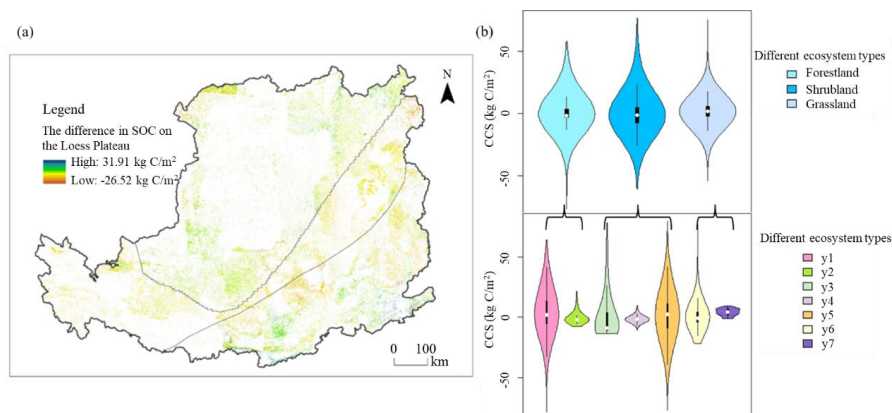


Forestland	SH		$y_1=0.3195 t+14.95 lat+$ $0.01356 ele - 0.00755 BIO4 -$ $4.02 BIO5+11 BIO10+$ $0.44 BIO13+1.791 BIO14 -$ $23.81 BIO15 - 1.686 BIO17-$ $632$	0.605	<0.05	21.831	17.209
	SA		$y_2=0.7384 t - 0.4148 BIO12+$ $4.2594 BIO14 - 0.8341 BIO17+$ $0.1456 BIO18+1.1633$	0.618	<0.01	9.039	7.001
Shrubland	WT	SH	$y_3=0.23 t^2 - 2.678 t - 1.221$	0.476	<0.01	34.814	22.858
		SA	$y_4=0.1555 t - 1.4904 BIO1 -$ $0.1544 BIO17+15.3573$	0.773	<0.01	2.281	1.715
	MT	SA	$y_5=1.6059 t - 12.1498 BIO3+$ $0.0071 BIO4+0.7615 BIO13 -$ $1.2096 BIO16+523.89$	0.551	<0.05	48.965	36.664
Grassland	WT		$y_6=0.5457 t+31.412 BD+$ $4.463 BIO9 - 2.489 BIO11 -$ $2.238 BIO14+27.184 BIO15 -$ $72.97$	0.830	<0.01	8.659	7.112
		MT		$y_7=-0.0497 t^2+1.455 t - 4.84$	0.790	<0.01	4.114

### 234 3.4 Mapping CCS

235 According to the regression models for CCS and the distribution of retired farmlands, the CCS in the retired farmlands  
 236 on the Loess Plateau was calculated (Fig. 7 a). The total benefit in CCS on the Loess Plateau was 21.77 Tg C with a range  
 237 between -26.52 and 31.91 kg C/m<sup>2</sup> at 30 m raster level. The potential CCS by different ecosystem types changed  
 238 significantly (Fig. 7 b, Table 2). Grasslands contributed the most CCS increment (17.657 Tg C). Among the different  
 239 climatic zones for grasslands, MT zone contributed the most (78.04%, -0.48–3.04 kg C/m<sup>2</sup>), followed by WT zone (21.96%,  
 240 -8.20–31.91 kg C/m<sup>2</sup>). Forestlands contributed the second largest CCS (2.429 Tg C) with 151.96% from SH zone  
 241 (-26.52–22.86 kg C/m<sup>2</sup>), and -51.96% from SA zone (-2.96–8.67 kg C/m<sup>2</sup>). The shrublands only contributed 7.74% of the  
 242 total benefit of carbon storage (1.685 Tg C) with 78.04% from MT-SA zone (-26.49–30.57 kg C/m<sup>2</sup>), 45.07% from WT-SA  
 243 zone (-4.00–3.28 kg C/m<sup>2</sup>) and -23.11% from WT-SH zone (-4.60–26.10 kg C/m<sup>2</sup>).

244 The potential CCS by different provinces also changed significantly, but the potential CCS in different ecosystem types  
 245 by the same provinces were evenly changed (Table S3). CCS increased more in Shanxi and Shaanxi provinces, followed by  
 246 Henan, Gansu, Inner Mongolia and Ningxia, and less in Qinghai province.



247 **Figure 7. Spatial distribution of the CCS, (a) the distribution in the whole study area, and (b) raster level frequency of**  
 248 **CCS.**

249

**Table 2 The CCS (positive and negative portion) in retired farmlands in different ecosystem types  
 in different climatic zones (Tg C).**

zone \ type	MT-SA	WT-SA	WT-SH	Total by ecosystems			
Forestland	1.318	-2.255	0.627	-0.952	6.461	-2.770	2.429
Shrubland	8.502	-6.223	0.369	-1.563	4.868	-4.269	1.685
Grassland	14.543	-0.765	13.196	-5.239	3.545	-7.625	17.657
Total by zones	24.363	-9.243	14.193	-7.753	14.874	-14.664	21.770

250 **4. Discussion**

251 4.1 Distribution of Retired Farmlands

252 In consideration of the topographic complexity and vegetational variation on the retired farmlands, a large-scale retrieve  
 253 of retired farmland information from remote sensing images is challenging (Wei et al., 2021). For instance, farmlands and  
 254 grasslands have similar spectrum characteristics in spring and summer seasons and can be easily confounded (Estel et al.,  
 255 2015), which lead to inaccuracy in remote sensing image classification. The inaccuracy can be minimized by comparing with  
 256 multi-source high-resolution remote sensing images (Yan et al., 2023). In this study, although different vegetation types were  
 257 involved on the retired farmlands (e.g., forestland, shrubland and grassland), the accuracy in identifying retired farmlands  
 258 could high to 90% by combining visual interpretation of Landsat dataset, field observation, globeland30 database, and  
 259 ultra-high resolution images from Google Earth.

260 Farmland retirement is the main land use change driver on the Loess Plateau. As classified in this study, retired  
 261 farmlands on the Loess Plateau from 2000 to 2021 are unevenly distributed across different climatic zones, because of the  
 262 significant hilly and gully terrain in the study area (Huang et al., 2007; Wen et al., 2015). We focused on forestlands,  
 263 shrublands and grasslands from retired farmlands, and noticed that most forestlands were distributed in the SH zone due to  
 264 higher precipitation than the SA zone. Grasslands were more distributed in the MT zone than in the WT zone, due to the  
 265 temperature in the MT zone being more favorable for grasses than in the WT zone, and people may be more engaged in



266 pastoral activities in the WT zone. Shrublands were more distributed in the MT-SA zone than in the WT-SH zone because the  
267 WT-SH zone is more suited to forest growth, thus having high percentage of tree cover and relatively low distribution of  
268 shrub. In this study, grasslands accounted for a large proportion in retired farmlands on the Loess Plateau, but the increase in  
269 forestlands were more significant. Different patterns of retired farmlands among different years were mainly caused by  
270 policy orientation and farmers' willingness of participation. Within the studied period, the central government of China  
271 implemented two rounds of GFGP in 1999-2013 and 2014-present, respectively. High rates of retirement were observed at  
272 the beginning of every round due to promising subsidies. The farmers' willingness of participation reduced thereafter, and a  
273 significant number of farmers chose to reclaim the retired farmlands (Xie et al., 2023).

#### 274 4.2 Model development for CCS

275 Land use change due to GFGP can strongly affect SOC, and SOC tend to be lower in farmlands (Deng et al., 2014),  
276 which was proved in this study by comparing retired and adjacent unchanged farmlands. The benefits of CCS in the retired  
277 farmlands reveals a close relationship to the length of farmland retirement, although a slightly decrease of SOC may be  
278 observed in early stage of retirement due to land use change (Deng et al., 2017). Although in the studied period, all the  
279 vegetation types had constant increasing trend after the first few years, the upper limit will be reached when the ecosystem  
280 become mature and stable, as showed in grassland with a logarithmic relationship. Some retired farmlands with decreasing  
281 SOC were found, which could be explained by interchange of reclamation and retirement (Qiu et al., 2018), but the deeper  
282 mechanism is still need to be explored. Moreover, the high SOC in adjacent farmlands due to good agricultural practice  
283 could also offset the benefit of CCS from the GFGP (negative CCS was mostly found in farmland with high SOC).

284 Based on the statistical analysis (Fig. 4), the range of the CCS in grasslands was significantly smaller than that in  
285 forestlands and shrublands. This indicates the accumulation rate of SOC in grasslands was lower than that in forestlands and  
286 shrublands due to the low primary productive and the fine quality of grass litter for decomposition (Lukina et al., 2020),  
287 whereas woody litter contains more lignin and decomposes slowly (Xiao et al., 2022). Therefore, different models were  
288 developed according to vegetation types and climatic zones. Based on the models, the climate factors had significant effect  
289 on CCS besides the length of farmland retirement. Among the climatic factors, the models showed that CCS were more  
290 sensitive to precipitation-based bioclimatic factors (e.g., *BIO12-BIO19*). This is because most of the Loess Plateau is located  
291 in semi-arid and arid area with limited precipitation (Zhang et al., 2015). Moreover, increased precipitation and temperatures  
292 can enhance the decomposition of surface litter (Sharma and Sharma, 2022), and in turn reduce CCS.

#### 293 4.3 Benefits in CCS on the Loess Plateau

294 Under climate change, ecological restoration is an urgent need to improve the healthiness of degraded ecosystems (Liu  
295 et al., 2023; Yang et al., 2023). As a major benefit from ecological restoration, the increase in SOC (CCS) brings a lot of  
296 interests due to SOC is the major carbon pool in the ecosystems. To illustrate CCS from ecological restoration, only a  
297 comparison of restored and adjacent unrestored ecosystems should be persuasive (Francaviglia et al., 2019). Numbers of  
298 studies focusing on CCS in retired farmlands has been conducted on the Loess Plateau, and found an increasing CCS as a  
299 result of GFGP (Wang et al., 2021b), and the national SOC sequestration caused by retirement was estimated to be 14.46 Tg  
300 per year (Zhao et al., 2013). But they failed to make comparison with the adjacent farmlands. In this study, we analyzed the  
301 CCS of retired farmlands and adjacent in-use farmlands, and confirmed that the GFGP can provide significant amount of  
302 CCS on the Loess Plateau, although negative CCS was found in some areas.



303 Recently, studies have shown that SOC stocks in the GFGP region on the Loess Plateau increased by 20.18 Tg C  
304 between 1982 and 2017 (Li et al., 2022). The total CCS (21.77 Tg C) of retired farmlands on the Loess Plateau estimated in  
305 this study was slightly higher than that value, which proved that the results of this study are reliable. Although the  
306 mechanisms of CCS are different for different vegetation restoration types in different climatic zones, the rate of carbon  
307 sequestration was higher in warm and humid areas than in cold or arid areas because of high temperatures and sufficient  
308 precipitation-induced strong photosynthesis and rapid plant growth. However, long time carbon storage in soil is essential in  
309 mitigate climate change. The high turnover rate of SOC in warm and humid areas may limit the benefit in carbon storage  
310 than in arid and semi-arid regions (Sierra et al., 2017).

#### 311 4.4 Limitations and Uncertainties

312 Remote sensing images are widely used in studies of land use change because of their accuracy and timeliness. In this  
313 study, the use of Landsat dataset has practical feasibility to provide reliable distribution of retired farmlands. However, the  
314 Loess Plateau has a large spatial area, and has a fragmented and complex topography, which increases the difficulty of land  
315 use classification. Therefore, the 30m resolution image can result in misclassification, although we obtained acceptable  
316 accuracy (80%–91%). Recently, the availability of ultra-high resolution images (sub-meter resolution) allows a more  
317 accurate classification, but lacks of long period records.

318 In this study, the direct comparison of retired farmlands and adjacent farmlands reflected a more persuasive CCS. The  
319 multivariate linear regression models that developed for estimating CCS can reduce the estimation error in the consideration  
320 of the spatial heterogeneity on the Loess Plateau. However, to predict the future potential of soil carbon sequestration in the  
321 retired farmlands on the Loess Plateau, the assistant of process-based ecosystem models could be more reliable, such as  
322 DLEM (Dynamic Land Ecosystem Model, (Tian et al., 2003)), LPJ-GUESS (Lund Potsdam Jena General Ecosystem  
323 Simulator, (Smith et al., 2001)), and CENTURY (Parton et al., 1987)

#### 324 5. Conclusions

325 Farmland retirement is an effective strategy to restore degraded ecosystem and increase carbon storage on the Loess  
326 Plateau. In this study, we found the total area of retired farmlands on the Loess Plateau during the study period was 39,065  
327 km<sup>2</sup>. The dominant ecosystem type was grasslands, followed by shrublands and forestlands. The area of retired farmlands  
328 showed significant interannual changes without a specific trend, and the retired farmlands varied in different climate zones.  
329 Area of retired farmlands in the MT-SA zone were significantly higher than WT-SA zone and WT-SH zone. Based on soil  
330 samples, we found that CCS increased with the length of farmland retirement, and developed seven regression models for  
331 CCS by length of farmland retirement, temperature, precipitation, soil bulk density, latitude and longitude, and ecosystem  
332 types. According to the models, the total benefits in CCS from retired farmlands on the Loess Plateau were estimated to be  
333 21.77 Tg C, with the variation ranged from -26.52 to 31.91 kg C/m<sup>2</sup> at grid cell level. The most CCS were contributed by  
334 retired farmlands in the MT-SA zone (15.120 Tg C), followed by WT-SA zone (6.440 Tg C) and WT-SH zone (0.210 Tg C).  
335 Therefore, Long-term implementation of GFGP brought significant impacts on increasing soil carbon sinks on the Loess  
336 Plateau, which contributed significantly in mitigating climate changes and promoting sustainability in the studied area.

#### 337 Competing interests

338 The authors declare no competing interests.

#### 339 Data availability



340 The associated datasets are available at Figshare (<https://doi.org/10.6084/m9.figshare.28785971>, Yang, 2025), including  
341 distribution of retired farmlands from 2000 to 2021, length of farmland retirement, and high resolution CCS from the retired  
342 farmlands.

#### 343 **Author contribution**

344 BG: data curation, investigation, methodology, formal analysis, validation and visualization; MF: investigation, formal  
345 analysis and validation; LY: data curation; TG, CM, XH, ZG, ZM: resources and visualization; QL: funding acquisition and  
346 conceptualization; ZW: resources; WL: Conceptualization, methodology, project administration and supervision. BG and  
347 WL: Writing – original draft preparation; All authors: Writing – review & editing.

#### 348 **Acknowledgements**

349 This study was funded by the National Key Research and Development Program of China (2022YFF1302200). The  
350 authors would like to thank all the reviewers who participated in the review.

#### 351 **Reference**

- 352 Calmon, M., Brancalion, P. H., Paese, A., Aronson, J., Castro, P., da Silva, S. C., and Rodrigues, R. R.: Emerging threats and  
353 opportunities for large-scale ecological restoration in the Atlantic Forest of Brazil, *Restor. Ecol.*, 19, 154-158,  
354 <https://doi.org/10.1111/j.1526-100X.2011.00772.x>, 2011.
- 355 Cui, W., Liu, J., Jia, J., and Wang, P.: Terrestrial ecological restoration in China: identifying advances and gaps, *Environ. Sci.*  
356 *Eur.*, 33, 1-14, <https://doi.org/10.1186/s12302-021-00563-2>, 2021.
- 357 de Oliveira Faria, C. and Magrini, A.: Biodiversity Governance from a Cross-Level and Cross-Scale Perspective: The case of  
358 the Atlantic Forest biome in Brazil, *Environm. Policy Govern.*, 26, 468-481, <https://doi.org/10.1002/eet.1728>, 2016.
- 359 Deng, L., Liu, G. b., and Shangguan, Z. p.: Land-use conversion and changing soil carbon stocks in C hina's  
360 'Grain-for-Green' Program: a synthesis, *Global Change Biol.*, 20, 3544-3556, <https://doi.org/10.1111/gcb.12508>, 2014.
- 361 Deng, L., Liu, S., Kim, D. G., Peng, C., Sweeney, S., and Shangguan, Z.: Past and future carbon sequestration benefits of  
362 China's grain for green program, *Global Environm. Change*, 47, 13-20, <https://doi.org/10.1016/j.gloenvcha.2017.09.006>,  
363 2017.
- 364 Estel, S., Kuemmerle, T., Alcántara, C., Levers, C., Prishchepov, A., and Hostert, P.: Mapping farmland abandonment and  
365 recultivation across Europe using MODIS NDVI time series, *Remote Sens. Environ.*, 163, 312-325,  
366 <https://doi.org/10.1016/j.rse.2015.03.028>, 2015.
- 367 Feng, X., Fu, B., Lu, N., Zeng, Y., and Wu, B.: How ecological restoration alters ecosystem services: an analysis of carbon  
368 sequestration in China's Loess Plateau, *Sci. Rep.*, 3, 2846, <https://doi.org/10.1038/srep02846>, 2013.
- 369 Ferreira, C. S., Seifollahi-Aghmiuni, S., Destouni, G., Ghajarnia, N., and Kalantari, Z.: Soil degradation in the European  
370 Mediterranean region: Processes, status and consequences, *Sci. Total Environ.*, 805, 150106,  
371 <https://doi.org/10.1016/j.scitotenv.2021.150106>, 2022.
- 372 Francaviglia, R., Álvaro-Fuentes, J., Di Bene, C., Gai, L., Regina, K., and Turtola, E.: Diversified arable cropping systems  
373 and management schemes in selected European regions have positive effects on soil organic carbon content, *Agriculture*,  
374 9, 261, <https://doi.org/10.3390/agriculture9120261>, 2019.
- 375 Graham, F.: Daily briefing: How to shore up Africa's Great Green Wall, *Nature*, <https://doi.org/10.1038/d41586-022-01247-4>,  
376 2022.
- 377 Huang, M., Gong, J., Shi, Z., Liu, C., and Zhang, L.: Genetic algorithm-based decision tree classifier for remote sensing  
378 mapping with SPOT-5 data in the HongShiMao watershed of the loess plateau, China, *Neural. Comput. Appl.*, 16,  
379 513-517, <https://doi.org/10.1007/s00521-007-0104-z>, 2007.
- 380 Lengefeld, E., Metternicht, G., and Nedungadi, P.: Behavior change and sustainability of ecological restoration projects,  
381 *Restor. Ecol.*, 28, 724-729, <https://doi.org/10.1111/rec.13159>, 2020.
- 382 Li, H., Wu, Y., Liu, S., Zhao, W., Xiao, J., Winowiecki, L. A., Vågen, T.-G., Xu, J., Yin, X., and Wang, F.: The  
383 Grain-for-Green project offsets warming-induced soil organic carbon loss and increases soil carbon stock in Chinese



- 384 Loess Plateau, *Sci. Total Environ.*, 837, 155469, <https://doi.org/10.1016/j.scitotenv.2022.155469>, 2022.
- 385 Liu, C., Jia, X., Ren, L., Zhao, C., Yao, Y., Zhang, Y., and Shao, M. a.: Cropland-to-shrubland conversion reduces soil water  
386 storage and contributes little to soil carbon sequestration in a dryland area, *Agric., Ecosyst. Environ.*, 354, 108572,  
387 <https://doi.org/10.1016/j.agee.2023.108572>, 2023.
- 388 Lu, F., Hu, H., Sun, W., Zhu, J., Liu, G., Zhou, W., Zhang, Q., Shi, P., Liu, X., and Wu, X.: Effects of national ecological  
389 restoration projects on carbon sequestration in China from 2001 to 2010, *Proc. Nat. Acad. Sci.*, 115, 4039-4044,  
390 <https://doi.org/10.1073/pnas.1700294115>, 2018.
- 391 Lukina, N., Kuznetsova, A., Tikhonova, E., Smirnov, V., Danilova, M., Gornov, A., Bakhmet, O., Kryshen, A., Tebenkova,  
392 D., and Shashkov, M.: Linking forest vegetation and soil carbon stock in Northwestern Russia, *Forests*, 11, 979,  
393 <https://doi.org/10.3390/f11090979>, 2020.
- 394 Ma, R., Wang, D., Cui, X., Yao, X., Li, S., Wang, H., and Liu, B.: Distribution and driving force of water use efficiency  
395 under vegetation restoration on the Loess Plateau, *Remote Sens.*, 14, 4513, <https://doi.org/10.3390/rs14184513>, 2022.
- 396 Macia, E., Allouche, J., Sagna, M. B., Diallo, A. H., Boëtsch, G., Guisse, A., Sarr, P., Cesaro, J.-D., and Duboz, P.: The Great  
397 Green Wall in Senegal: questioning the idea of acceleration through the conflicting temporalities of politics and nature  
398 among the Sahelian populations, *Ecol. Society*, 28, 31, <https://doi.org/10.5751/ES-13937-280131>, 2023.
- 399 Mir, Y. H., Ganie, M. A., Shah, T. I., Aezum, A. M., Bangroo, S. A., Mir, S. A., Dar, S. R., Mahdi, S. S., Baba, Z. A., and  
400 Shah, A. M.: Soil organic carbon pools and carbon management index under different land use systems in North western  
401 Himalayas, *PeerJ*, 11, e15266, <https://doi.org/10.7717/peerj.15266>, 2023.
- 402 Ouyang, Z., Zheng, H., Xiao, Y., Polasky, S., Liu, J., Xu, W., Wang, Q., Zhang, L., Xiao, Y., and Rao, E.: Improvements in  
403 ecosystem services from investments in natural capital, *Science*, 352, 1455-1459, <https://doi.org/10.1126/science.aaf2295>,  
404 2016.
- 405 Pape, T.: Futuristic restoration as a policy tool for environmental justice objectives, *Restor. Ecol.*, 30, e13629,  
406 <https://doi.org/10.1111/rec.13629>, 2022.
- 407 Parton, W. J., Schimel, D. S., Cole, C. V., and Ojima, D. S.: Analysis of factors controlling soil organic matter levels in Great  
408 Plains grasslands, *Soil Sci. Soc. Am. J.*, 51, 1173-1179, <https://doi.org/10.2136/sssaj1987.03615995005100050015x>,  
409 1987.
- 410 Paustian, K., Collier, S., Baldock, J., Burgess, R., Creque, J., DeLonge, M., Dungait, J., Ellert, B., Frank, S., and Goddard, T.:  
411 Quantifying carbon for agricultural soil management: from the current status toward a global soil information system,  
412 *Carbon Manage.*, 10, 567-587, <https://doi.org/10.1080/17583004.2019.1633231>, 2019.
- 413 Piffer, P. R., Calaboni, A., Rosa, M. R., Schwartz, N. B., Tambosi, L. R., and Uriarte, M.: Ephemeral forest regeneration  
414 limits carbon sequestration potential in the Brazilian Atlantic Forest, *Global Change Biol.*, 28, 630-643,  
415 <https://doi.org/10.1111/gcb.15944>, 2022.
- 416 Prăvălie, R., Patriche, C., Borrelli, P., Panagos, P., Roșca, B., Dumitrașcu, M., Nita, I.-A., Săvulescu, I., Birsan, M.-V., and  
417 Bandoc, G.: Arable lands under the pressure of multiple land degradation processes. A global perspective, *Environ. Res.*,  
418 194, 110697, <https://doi.org/10.1016/j.envres.2020.110697>, 2021.
- 419 Qiu, B., Zou, F., Chen, C., Tang, Z., Zhong, J., and Yan, X.: Automatic mapping afforestation, cropland reclamation and  
420 variations in cropping intensity in central east China during 2001–2016, *Ecol. Indic.*, 91, 490-502,  
421 <https://doi.org/10.1016/j.ecolind.2018.04.010>, 2018.
- 422 Scharlemann, J. P., Tanner, E. V., Hiederer, R., and Kapos, V.: Global soil carbon: understanding and managing the largest  
423 terrestrial carbon pool, *Carbon Manage.*, 5, 81-91, <https://doi.org/10.4155/cmt.13.77>, 2014.
- 424 Shao, M., Adnan, M., Zhang, L., Liu, P., Cao, J., and Qin, X.: Carbonate mineral dissolution and its carbon sink effect in  
425 Chinese loess, *Land*, 12, 133, <https://doi.org/10.3390/land12010133>, 2022.
- 426 Sharma, G. and Sharma, L.: Climate change effect on soil carbon stock in different land use types in eastern Rajasthan, India,  
427 *Environm. Dev. Sustain.*, 24, 4942-4962, <https://doi.org/10.1007/s10668-021-01641-4>, 2022.
- 428 Sierra, C. A., Malghani, S., and Loescher, H. W.: Interactions among temperature, moisture, and oxygen concentrations in  
429 controlling decomposition rates in a boreal forest soil, *Biogeosciences*, 14, 703-710,  
430 <https://doi.org/10.5194/bg-14-703-2017>, 2017.



- 431 Smith, B., Prentice, I. C., and Sykes, M. T.: Representation of vegetation dynamics in the modelling of terrestrial ecosystems:  
432 comparing two contrasting approaches within European climate space, *Glob. Ecol. Biogeogr.*, 621-637,  
433 <https://doi.org/https://www.jstor.org/stable/3182691>, 2001.
- 434 Sun, Y., Zhu, J., Yan, Q., Hu, Z., and Zheng, X.: Changes in vegetation carbon stocks between 1978 and 2007 in central  
435 Loess Plateau, China, *Environ. Earth Sci.*, 75, 1-16, <https://doi.org/10.1007/s12665-015-5199-4>, 2016.
- 436 Tian, H., Melillo, J. M., Kicklighter, D. W., Pan, S., Liu, J., McGuire, A. D., and Moore III, B.: Regional carbon dynamics in  
437 monsoon Asia and its implications for the global carbon cycle, *Glob. Planet. Change*, 37, 201-217,  
438 [https://doi.org/10.1016/S0921-8181\(02\)00205-9](https://doi.org/10.1016/S0921-8181(02)00205-9), 2003.
- 439 Wang, J., Liu, Z., Gao, J., Emanuele, L., Ren, Y., Shao, M., and Wei, X.: The Grain for Green project eliminated the effect of  
440 soil erosion on organic carbon on China's Loess Plateau between 1980 and 2008, *Agric., Ecosyst. Environ.*, 322, 107636,  
441 <https://doi.org/10.1016/j.jclepro.2021.128161>, 2021a.
- 442 Wang, L., Li, Z., Wang, D., Chen, J., Liu, Y., Nie, X., Zhang, Y., Ning, K., and Hu, X.: Unbalanced social-ecological  
443 development within the Dongting Lake basin: Inspiration from evaluation of ecological restoration projects, *J. Cleaner  
444 Prod.*, 315, 128161, <https://doi.org/10.1016/j.agec.2021.107636>, 2021b.
- 445 Wei, Z., Gu, X., Sun, Q., Hu, X., and Gao, Y.: Analysis of the spatial and temporal pattern of changes in abandoned farmland  
446 based on long time series of remote sensing data, *Remote Sens.*, 13, 2549, <https://doi.org/10.3390/rs13132549>, 2021.
- 447 Wen, W., Wang, Y., Yang, L., Liang, D., Chen, L., Liu, J., and Zhu, A.-X.: Mapping soil organic carbon using auxiliary  
448 environmental covariates in a typical watershed in the Loess Plateau of China: a comparative study based on three  
449 kriging methods and a soil land inference model (SoLIM), *Environ. Earth Sci.*, 73, 239-251,  
450 <https://doi.org/10.1007/s12665-014-3518-9>, 2015.
- 451 Xiao, J.: Satellite evidence for significant biophysical consequences of the “Grain for Green” Program on the Loess Plateau  
452 in China, *J. Geophys. Res.:Biogeosci.*, 119, 2261-2275, <https://doi.org/10.1002/2014JG002820>, 2014.
- 453 Xiao, Y., Huang, Z., Ling, Y., Cai, S., Zeng, B., Liang, S., and Wang, X.: Effects of forest vegetation restoration on soil  
454 organic carbon and its labile fractions in the Danxia landform of China, *Sustainability*, 14, 12283,  
455 <https://doi.org/10.3390/su141912283>, 2022.
- 456 Xie, Y., Ma, Z., Fang, M., Liu, W., Yu, F., Tian, J., Zhang, S., and Yan, Y.: Analysis of Net Primary Productivity of Retired  
457 Farmlands in the Grain-for-Green Project in China from 2011 to 2020, *Land*, 12, 1078,  
458 <https://doi.org/10.3390/land12051078>, 2023.
- 459 Xu, C., Jiang, Y., Su, Z., Liu, Y., and Lyu, J.: Assessing the impacts of Grain-for-Green Programme on ecosystem services in  
460 Jinghe River basin, China, *Ecol. Indic.*, 137, 108757, <https://doi.org/10.1016/j.ecolind.2022.108757>, 2022.
- 461 Yan, X., Li, J., Smith, A. R., Yang, D., Ma, T., and Su, Y.: Rapid land cover classification using a 36-year time series of  
462 multi-source remote sensing data, *Land*, 12, 2149, <https://doi.org/10.1016/j.ecolind.2022.108757>, 2023.
- 463 Yang, Y., Sun, H., Zhang, P., Wu, F., Qiao, J., Li, T., Wang, Y., and An, S.: Review of managing soil organic C sequestration  
464 from vegetation restoration on the Loess Plateau, *Forests*, 14, 1964, <https://doi.org/10.3390/f14101964>, 2023.
- 465 Yang, . leilei .: The 30-meter resolution distribution of retired farmlands and their carbon sequestration on the Loess Plateau  
466 in China from 2000 to 2021, *Figshare[data set]*, <https://doi.org/10.6084/m9.figshare.28785971>, 2025.
- 467 Zhang, F., Li, C., Wang, Z., Glidden, S., Grogan, D. S., Li, X., Cheng, Y., and Frohling, S.: Modeling impacts of  
468 management on farmland soil carbon dynamics along a climate gradient in Northwest China during 1981–2000, *Ecol.  
469 Modell.*, 312, 1-10, <https://doi.org/10.1016/j.ecolmodel.2015.05.006>, 2015.
- 470 Zhang, K., Yihe, L., Bojie, F., and Ting, L.: The effects of restoration on vegetation trends: spatiotemporal variability and  
471 influencing factors, *Earth Environ. Sci. Trans. R. Soc. Edinburgh*, 109, 473-481,  
472 <https://doi.org/10.1017/S1755691018000518>, 2018.
- 473 Zhang, Q., Lu, J., Xu, X., Ren, X., Wang, J., Chai, X., and Wang, W.: Spatial and temporal patterns of carbon and water use  
474 efficiency on the loess plateau and their influencing factors, *Land*, 12, 77, <https://doi.org/10.3390/land12010077>, 2022.
- 475 Zhao, F., Chen, S., Han, X., Yang, G., Feng, Y., and Ren, G.: Policy-guided nationwide ecological recovery: Soil carbon  
476 sequestration changes associated with the Grain-to-Green Program in China, *Soil Sci.*, 178, 550-555,  
477 <https://doi.org/10.1097/SS.000000000000018>, 2013.



478 Zhou, R., Pan, X., Wei, H., Xie, X., Wang, C., Liu, Y., Li, Y., and Shi, R.: Soil organic carbon stocks in terrestrial ecosystems  
479 of China: revised estimation on three-dimensional surfaces, *Sustainability*, 8, 1003, <https://doi.org/10.3390/su8101003>,  
480 2016.  
481